PHYSICAL REVIEW D **76,** 043524 (2007)

Probing the nature of dark matter with cosmic x rays: Constraints from "dark blobs" and grating spectra of galaxy clusters

Signe Riemer-Sorensen,[1] Kristian Pedersen,[1] Steen H. Hansen,[1] and Haakon Dahle[2]

[1]*Dark Cosmology Centre, Niels Bohr Institute, University of Copenhagen, Juliane Maries Vej 30, DK-2100 Copenhagen, Denmark*
[2]*Institute of Theoretical Astrophysics, University of Oslo, P.O. Box 1029, Blindern, N-0315 Oslo, Norway*

(Received 2 October 2006; revised manuscript received 30 May 2007; published 28 August 2007)

Gravitational lensing observations of galaxy clusters have identified dark matter blobs with remarkably low baryonic content. We use such a blob to probe the particle nature of dark matter with x-ray observations. From these observations we improve the most conservative constraints from the Milky Way halo on a particular dark matter candidate, the sterile neutrino, by an order of magnitude. We also study high resolution x-ray grating spectra of a cluster of galaxies. Based on these conservative constraints obtained from cosmic x-ray observations alone, the low mass ($m_s \lesssim 10$ keV) and low mixing angle ($\sin^2(2\theta) \lesssim 10^{-6}$) sterile neutrino is still a viable dark matter candidate.

DOI: 10.1103/PhysRevD.76.043524 PACS numbers: 95.35.+d, 14.60.St, 95.85.Nv, 98.65.Cw

I. INTRODUCTION

The cosmological dark matter abundance is firmly established through observations of the cosmic microwave background and of the large scale structure of the Universe [1,2]. This is complemented by measurements of dark matter on smaller scales by studies of, e.g. the rotation curves of galaxies, gravitational lensing by galaxies and clusters of galaxies [3], the velocity dispersion of galaxies in clusters of galaxies, and x ray emitting hot gas in clusters of galaxies [4]. However, the particle nature of dark matter remains a puzzle.

There are numerous dark matter candidates, among which the sterile neutrino is particularly well motivated. The sterile neutrino is a natural dark matter candidate in a minimally extended standard model of particle physics [5] and it provides solutions to other problems: the masses of the active neutrinos [6], the baryon asymmetry of the Universe [7], and the observed peculiar velocities of pulsars [8,9]. Sterile neutrinos participate in the flavor-mass eigenstate oscillations of the active standard model neutrinos, and are thereby allowed to decay radiatively through a two-body decay with photon energy predicted to lie in the x-ray range ($E_\gamma = m_s/2$, where m_s is the rest mass of the sterile neutrino). This renders it a testable dark matter candidate [10].

The decay rate of any dark matter candidate with a radiative two-body decay can be constrained from observations of dark matter concentrations (for references see [11–18]). The strongest constraints are obtained from studying dark matter dominated regions, and with instruments with high spectral resolution since the decay line is expected only to suffer negligible broadening due to motion of the dark matter. The velocity dispersion of the dark matter in clusters of galaxies can be found from x-ray observations by solving the hydrostatic equation and the Jeans equations. The resulting velocity dispersion has a peak of the order of 500 km/s, which leads to a line broadening that is negligible compared to the instrumental spectral resolution.

Recent gravitational lensing observations of the mass distribution in merging galaxy cluster systems [19,20] have identified cluster scale dark matter "blobs" with very low baryonic content. This allows for the novel possibility of using such almost pure dark matter blobs to probe the particle nature of the dark matter [21]. Below we analyze x-ray observations of the dark matter blob in the cluster of galaxies Abell 520. Also, we investigate the possibility of using high resolution x-ray grating spectra with the cluster of galaxies Abell 1835 as a generic example. Throughout this work a cosmology with $\Omega_m = 0.26$, $\Omega_\Lambda = 0.74$, $H_0 = 100\ h\,\mathrm{km\,sec^{-1}\,Mpc^{-1}} = 71\,\mathrm{km\,sec^{-1}\,Mpc^{-1}}$ is assumed.

II. X-RAY DATA ANALYSIS

When a spectrum of a given dark matter dense region has been obtained from an observation through standard data processing with CIAO version 3.3 [22], there are different ways of searching for a hypothetical monoenergetic emission line and to determine an upper limit on the flux from decaying dark matter particles. The simplest and most conservative method is the "slice method," where the energy range of the spectrum is divided into bins of a width equal to the instrumental energy resolution (2σ), and all of the x-ray flux in a particular bin is determined from a model fitted to the spectrum. The slice method is very robust, as the physics behind the fitted model is irrelevant, and the method does not require any assumptions about the x-ray background, but regards all received flux as an upper limit for the flux from decaying dark matter. This is despite the fact that the total flux is known to consist of several contributions: the cosmic x-ray background from unresolved sources, the x-ray emission from the intracluster medium, the Milky Way halo, and the instrumental background. The "slice method" takes into account that an emission line from decaying dark matter could "hide" under a line feature in the spectrum [14]. The flux obtained

with the slice method is almost identical to the flux obtained by giving the slice the shape of a Gaussian centered at the slice energy, and with the width σ and the maximum at the value of the model fitted to the spectrum. Other methods for constraining the flux (for example [13,15]) can give stronger, but less conservative or robust, results. For a discussion of different methods see [23]. In this study, we conservatively use the slice method.

III. THE DARK MATTER BLOB IN THE GALAXY CLUSTER ABELL 520

For direct imaging data, the field of view can be optimized by observing a dark matter dense region with low x-ray emission, from baryons. A unique example is the merging cluster of galaxies Abell 520 [24] containing a ''blob'' of high mass concentration with very low x-ray emission discovered recently using weak gravitational lensing; see Fig. 1 [25]. The luminosity distance to A520 is $D_L = 980$ Mpc ($z = 0.203$, [26]).

An ACIS-S3 0.3–9.0 keV spectrum was extracted from the 67 ks *Chandra* observation (observation id 4215) for a region centered at the dark blob with a radius of $r = 0.85$ arcmin $= 190$ kpc (the red circle in Fig. 1). A non-physical model consisting of a power law and six Gaussians designed to fit the spectrum was fitted to the spectrum with a reduced χ^2 of 1.2 (for 80 degrees of freedom). The extracted spectrum and the fitted model are shown in Fig. 2

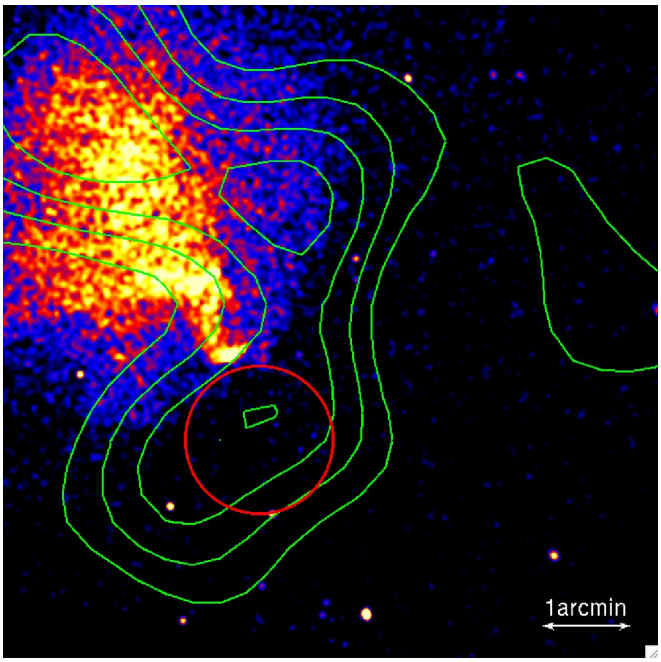

FIG. 1 (color online). Abell 520 observed in x rays (0.3–10.0 keV) with *Chandra* and contours of the gravitational potential determined from weak lensing overlaid. The dark matter blob in the circle has very low x-ray emission from baryons.

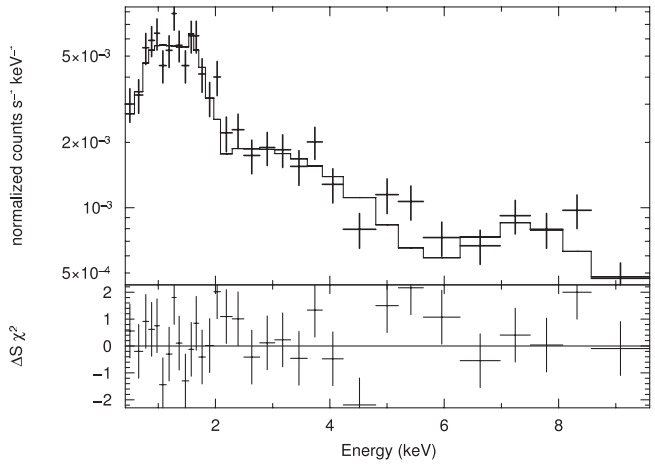

FIG. 2. The extracted spectrum of Abell 520 and the fitted model (upper panel) and the fit residuals (lower panels).

The flux was determined using the slice method for a slice width given by the energy resolution of ACIS-S3 [27]:

$$\sigma_{S3} = 0.005E_\gamma + 0.05 \text{ keV}. \quad (1)$$

The mass of the dark matter blob in Abell 520 has been derived from weak gravitational lensing to be $M_{\text{fov}}^{\text{blob}} = 4.78 \pm 1.5 \times 10^{13} h^{-1} \text{M}_\odot$. This value is based on measuring the overdensity in the region in the red circle (Fig. 1) with respect to the mean density in a surrounding annulus with inner and outer radius of 0.85 arcmin and 4 arcmin, respectively. Hence, the mass value can be regarded as a conservative lower limit on the mass contained within the blob region. A mass map generated using the method of [28] shows a 4σ detection of mass in this region, compared to ''noise'' maps based on randomized shear values. A detailed description of the data and methodology of the weak lensing analysis is given elsewhere [29]. An independent weak lensing analysis of Abell 520 [30] confirms the existence of the blob, centered at a slightly different position. The offset between the two centers is approximately 0.5 arcmin. The blob region used here contains a significant amount of dark matter according to both lensing observations.

The dominating baryonic component in clusters of galaxies is the hot x ray emitting intracluster gas. However the generally observed gas mass fraction is only $f_{\text{gas}} \approx 0.11$ [31]. In merging galaxy cluster systems, the gas has been displaced from the blob regions, so the gas mass is negligible and the mass of the dark matter is taken to be the total mass of the blobs determined from gravitational lensing.

IV. GRATING OBSERVATIONS

A good spectral resolution increases the sensitivity to a monoenergetic emission line. The high spatial resolution of the *Chandra* x-ray telescope can be turned into a very

high spectral resolution (≈ 5 eV) by deflecting the incoming photons in a grating, as the deflection angle is highly sensitive to the photon energy. The ACIS-HETG instrument consists of two gratings, which on demand can be placed between the mirrors and the ACIS CCDs: the high energy grating, 0.8–9.0 keV, and the medium energy grating, 0.4–5.0 keV [27].

When the incoming photons are deflected in a grating, the information of their spatial origin is lost. This makes it impossible to optimize the ratio of expected dark matter signal to noise from x ray emitting baryons in the observational field of view (as described by [13–16]). The spectral resolution of a grating spectrometer decreases proportionally to the angular extension of the source. In order to determine whether the gratings improve the resolution, the grating effects of extended sources were investigated. Any spatially extended source can be thought of as a collection of point sources. The deflection angle, χ, of photons from a monoenergetic point source with incoming angle θ, is given by the grating equation:

$$n\lambda = d(\sin(\theta) - \sin(\chi)), \tag{2}$$

where n is the deflection order, and d the grating distance. A range of combinations of values for λ and θ leads to the same deflection angle. Let χ_0 be a given (fixed) deflection angle. If χ_0 corresponds to an on-axis source, only one set of values for $(\lambda, \theta) = (\lambda_0, 0)$ is valid and χ_0 is given as $n\lambda_0 = -d\sin\chi_0$. The values of (λ, θ) corresponding to this deflection angle is given by

$$\lambda = \frac{d}{n}\sin\theta + \lambda_o n, \tag{3}$$

$$= \frac{b}{D_L}(1+z)^2\frac{d}{n} + \lambda_o n, \tag{4}$$

where the last equality is for a monoenergetic point source with an off-axis projected distance, b. D_L is the source luminosity distance, and z is the redshift. For a monoenergetic source with a given mass distribution, the flux originating at each θ should be weighted according to the mass at the given projected radius. An example of the weighting is shown in Fig. 3 for a Navarro-Frenk-White profile for Abell 1835. The following values have been adopted for Abell 1835: a luminosity distance of $D_L = 1225$ Mpc ($z = 0.252$, [32]), a scale radius of $r_s \approx 800$ kpc corresponding to 4.2 arcmin [33], and a mass within the scale radius of $M_s = 6.5 \times 10^{14}\mathrm{M}_\odot$ [33]. The resolution is given by the full width half maximum of the resulting distribution.

It turns out that the obtained energy dependent resolution ($\sigma_{\mathrm{HEG}} \approx 1.5$ keV for a photon energy of 1 keV) is of the same order of magnitude as the imaging spectral resolution given by Eq. (1) for realistic dark matter structures. In order to improve the existing constraints by orders of magnitude, a new class of very sensitive x-ray instruments with a high spectral resolution is needed (see also [34]).

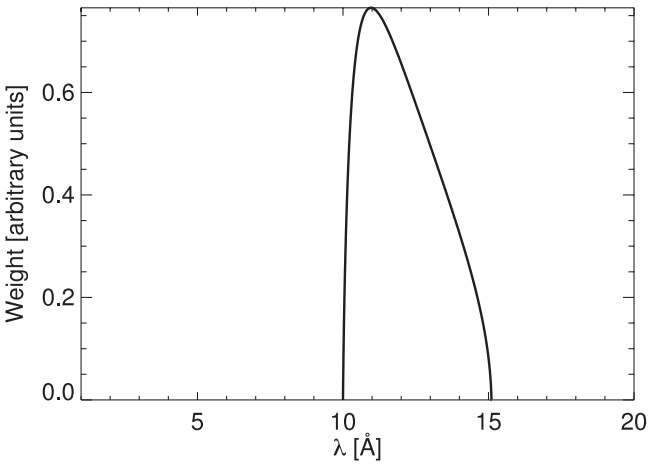

FIG. 3. An example of the weighting given by Eq. (3) for a Navarro-Frenk-White profile for Abell 1835.

V. DECAY RATE

Let us now consider a specific dark matter candidate, the sterile neutrino. This can decay radiatively as $\nu_s \rightarrow \nu_\alpha + \gamma$, where ν_α is an active neutrino. This is a two-body decay with a photon energy of $E_\gamma = m_s/2$. Assuming only one kind of dark matter, the observed flux, F_{obs}, at a given photon energy yields an upper limit on the decay rate from two-body radiatively decaying dark matter:

$$\Gamma_\gamma \leq \frac{8\pi F_{\mathrm{obs}} D_L^2}{M_{\mathrm{fov}}}. \tag{5}$$

The determined flux is dominated by the background, which varies with energy, introducing an apparent mass dependence.

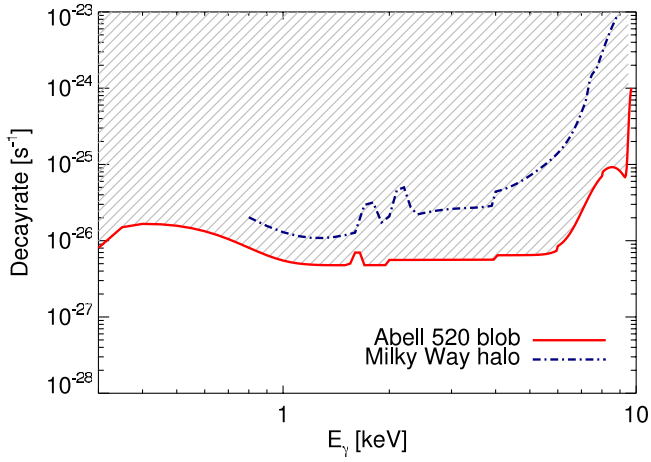

FIG. 4 (color online). The upper limit on the radiative two-body decay rate obtained from the dark matter blob of Abell 520 (solid) together with the Milky Way halo constraint [14] (dot-dashed).

The Milky Way dark matter halo will always be included in the observation, but its mass contribution to the total mass in the field of view divided by its mean luminosity distance squared is negligible compared to the same ratio for the dark matter blob.

Figure 4 shows the very general upper limit on the decay rate of any dark matter candidate [given by Eq. (5)] obtained from the total amount of received flux for the Abell 520 dark matter blob. It is seen that the obtained constraints are an order of magnitude stronger than the constraints obtained from observations of the Milky Way halo alone [14,15].

VI. CONSTRAINING MASS AND MIXING ANGLE

By regarding all decay branches possible through oscillations, the mean lifetime of a sterile Dirac neutrino of mass, m_s, has been determined to be [35,36]

$$\tau = \frac{1}{\Gamma_{\rm tot}} = \frac{f(m_s)\cdot 10^{20}}{(m_s/{\rm kev})^5 \sin^2(2\theta)}\ {\rm sec}^{-1}, \qquad (6)$$

where $\Gamma_{\rm tot}$ is the total decay rate. $f(m_s)$ takes into account the open decay channels so that for $m_s < 1$ MeV, where only the neutrino channel is open, $f(m_s) = 0.86$. For Majorana neutrinos, which we will be considering below, $f(m_s)$ is half the value for Dirac neutrinos. The branching ratio of the radiative decay is $\Gamma_\gamma/\Gamma_{\rm tot} = 27\alpha/8\pi \approx 1/128$ [35]. This can be combined with Eq. (5) to give

$$\sin^2(2\theta) \lesssim 7\times 10^{17}\ {\rm sec}^{-1}\left(\frac{F_{\rm det}}{{\rm erg/cm^2/sec}}\right)\left(\frac{m_s}{\rm keV}\right)^{-5} \times \left[\frac{(M_{\rm fov}/{\rm M}_\odot)}{(D_L/{\rm Mpc})^2}\right]^{-1}. \qquad (7)$$

The observational constraints in the $\sin^2(2\theta) - m_s$ parameter space are shown in Fig. 5 for the dark matter blob of Abell 520 (red) together with the Tremaine-Gunn limit (hatched, [37]) and earlier x-ray constraints (gray, [13–18,38]). The constraints derived here are very robust as they have been derived from the total amount of received x-ray flux without subtraction of any background contributions.

In the simplest Dodelson-Widrow production scenario of the sterile neutrinos [5], lower mass bounds on the mass can be obtained from studies of the Ly-α forest [39–41], which combined with the x-ray constraints rule out the full parameter space. However, there are other production scenarios, for example, via inflation [42], for which the Ly-α results cannot be applied.

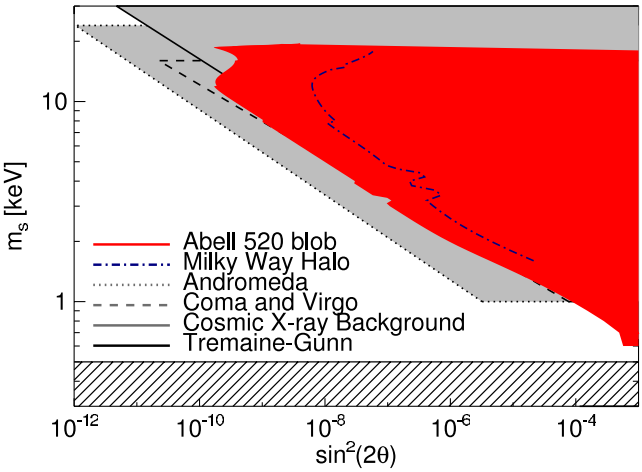

FIG. 5 (color online). The observational constraints from the dark matter blob of Abell 520 (red/dark) together with the Tremaine-Gunn limit (hatched, [37]) and earlier x-ray constraints (gray, [13–18,38]).

VII. CONCLUSIONS

A very general constraint on the decay rate for all dark matter particle candidates with a two-body radiative decay in the x-ray range has been derived. We have analyzed a spectrum obtained through direct imaging of the almost pure dark matter blob in the galaxy cluster Abell 520 and explored the possibility of using x-ray grating data in order to improve the resolution. The mass and mixing angle can be constrained in the specific case of sterile neutrinos, leaving a low mass ($m_s \lesssim 10$ keV) and low mixing angle ($\sin^2(2\theta) \lesssim 10^{-6}$) window open.

The obtained constraints can be improved significantly by improving the signal to noise ratio (optimization of field of view) and by improving the instrumental spectral resolution. Unfortunately, x-ray gratings are not particular suited for observations of extended dark matter structures such as clusters of galaxies as the resolution decreases with the source extension. In order to improve the existing constraints by orders of magnitudes, a new class of very sensitive x-ray instruments with a high spectral resolution is needed (see also [43]).

ACKNOWLEDGMENTS

The Dark Cosmology Centre is funded by the Danish National Research Foundation. K. P. acknowledges support from the Instrument Center for Danish Astrophysics. We thank M. Shaposhnikov for pleasant and useful discussions, and A. Boyarsky and O. Ruchayskiy for useful comments.

[1] D. N. Spergel *et al.* (WMAP Collaboration), Astrophys. J. Suppl. Ser. **148**, 175 (2003).

[2] U. Seljak *et al.* (SDSS Collaboration), Phys. Rev. D **71**, 103515 (2005).

[3] P. Schneider, arXiv:astro-ph/0306465.

[4] P. Rosati, S. Borgani, and C. Norman, Annu. Rev. Astron. Astrophys. **40**, 539 (2002).

[5] S. Dodelson and L. M. Widrow, Phys. Rev. Lett. **72**, 17 (1994).

[6] T. Asaka, S. Blanchet, and M. Shaposhnikov, Phys. Lett. B **631**, 151 (2005).

[7] T. Asaka and M. Shaposhnikov, Phys. Lett. B **620**, 17 (2005).

[8] G. M. Fuller, A. Kusenko, I. Mocioiu, and S. Pascoli, Phys. Rev. D **68**, 103002 (2003).

[9] A. Kusenko and G. Segre, Phys. Lett. B **396**, 197 (1997).

[10] A. D. Dolgov and S. H. Hansen, Astropart. Phys. **16**, 339 (2002).

[11] K. Abazajian and S. M. Koushiappas, Phys. Rev. D **74**, 023527 (2006).

[12] K. N. Abazajian, M. Markevitch, S. M. Koushiappas, and R. C. Hickox, Phys. Rev. D **75**, 063511 (2007).

[13] C. R. Watson, J. F. Beacom, H. Yuksel, and T. P. Walker, Phys. Rev. D **74**, 033009 (2006).

[14] S. Riemer-Sorensen, S. H. Hansen, and K. Pedersen, Astrophys. J. **644**, L33 (2006).

[15] A. Boyarsky, A. Neronov, O. Ruchayskiy, and M. Shaposhnikov, Phys. Rev. D **74**, 103506 (2006).

[16] A. Boyarsky, A. Neronov, O. Ruchayskiy, M. Shaposhnikov, and I. Tkachev, Phys. Rev. Lett. **97**, 261302 (2006).

[17] A. Boyarsky, J. Nevalainen, and O. Ruchayskiy, arXiv:astro-ph/0610961.

[18] A. Boyarsky, O. Ruchayskiy, and M. Markevitch, arXiv:astro-ph/0611168.

[19] D. Clowe, M. Bradac, A. H. Gonzalez, M. Markevitch, S. W. Randall, C. Jones, and D. Zaritsky, arXiv:astro-ph/0608407.

[20] H. Dahle, K. Pedersen, P. B. Lilje, S. J. Maddox, and N. Kaiser, Astrophys. J. **591**, 662 (2003).

[21] S. H. Hansen, J. Lesgourgues, S. Pastor, and J. Silk, Mon. Not. R. Astron. Soc. **333**, 544 (2002).

[22] A. Fruscione *et al.*, Chandra Interactive Analysis of Observations (CIAO), 2006, http://cxc.harvard.edu/ciao/.

[23] S. Riemer-Sorensen, MSc thesis, University of Copenhagen, 2006.

[24] M. Markevitch, F. Govoni, G. Brunetti, and D. Jerius, Astrophys. J. **627**, 733 (2005).

[25] A similar analysis of the dark matter concentration in the bullet cluster has been carried out by Boyarsky *et al.* Their findings are qualitatively similar to the blob results presented here [M. Shaposhnikov (private communication)].

[26] H. Ebeling *et al.*, Mon. Not. R. Astron. Soc. **301**, 881 (1998).

[27] The Chandra Proposers' Observatory Guide, Version 9.0, http://cxc.harvard.edu/proposer/POG/html; C. R. Canizares, Chandra High Energy Transmission Grating Spectrometer, http://space.mit.edu/CSR/hetg_info.html.

[28] N. Kaiser and G. Squires, Astrophys. J. **404**, 441 (1993).

[29] H. Dahle, N. Kaiser, R. J. Irgens, P. B. Lilje, and S. J. Maddox, Astrophys. J. Suppl. Ser. **139**, 313 (2002).

[30] N. Okabe and K. Umetsu, arXiv:astro-ph/0702649.

[31] S. W. Allen, A. C. Fabian, R. W. Schmidt, and H. Ebeling, Mon. Not. R. Astron. Soc. **334**, L11 (2002).

[32] R. W. Schmidt, S. W. Allen, and A. C. Fabian, Mon. Not. R. Astron. Soc. **327**, 1057 (2001).

[33] L. M. Voigt and A. C. Fabian, Mon. Not. R. Astron. Soc. **368**, 518 (2006).

[34] A. Boyarsky, J. W. den Herder, A. Neronov, and O. Ruchayskiy, arXiv:astro-ph/0612219.

[35] V. D. Barger, R. J. N. Phillips, and S. Sarkar, Phys. Lett. B **352**, 365 (1995); **356**, 617(E) (1995).

[36] A. D. Dolgov, S. H. Hansen, G. Raffelt, and D. V. Semikoz, Nucl. Phys. **B590**, 562 (2000).

[37] S. Tremaine and J. E. Gunn, Phys. Rev. Lett. **42**, 407 (1979).

[38] A. Boyarsky, A. Neronov, O. Ruchayskiy, and M. Shaposhnikov, Mon. Not. R. Astron. Soc. **370**, 213 (2006).

[39] U. Seljak, A. Makarov, P. McDonald, and H. Trac, Phys. Rev. Lett. **97**, 191303 (2006).

[40] M. Viel, J. Lesgourgues, M. G. Haehnelt, S. Matarrese, and A. Riotto, Phys. Rev. D **71**, 063534 (2005).

[41] M. Viel, J. Lesgourgues, M. G. Haehnelt, S. Matarrese, and A. Riotto, Phys. Rev. Lett. **97**, 071301 (2006).

[42] M. Shaposhnikov and I. Tkachev, Phys. Lett. B **639**, 414 (2006).

[43] A. Boyarsky, J. W. den Herder, A. Neronov, and O. Ruchayskiy, arXiv:astro-ph/0612219.